A GPS-free Power Grid Monitoring System over Mobile Platforms

Haoyang Lu, Lingwei Zhan *Student Member, IEEE*, Yilu Liu, *Fellow, IEEE* and Wei Gao, *Member, IEEE*
Department of Electrical Engineering and Computer Science
University of Tennessee
Knoxville, TN, USA
Email:{hlu9,lzhan,liu,weigao}@utk.edu

***Abstract*—In smart grids, the deviation of frequency and phase angle serves as an important indicator of abnormal events, the detection of which is critical to maintain reliable and stable operations of the power grid. However, the high cost and low accessibility of current power grid monitoring systems restrict their large-scale deployment over highly distributed microgrids. In this paper, we present a practical frequency and phase angle monitoring system design over mobile platforms, which significantly reduces the cost of power grid monitoring by utilizing the functionalities of modern mobile devices. We harvest the 200 Hz Primary Synchronization Signal (PSS) embedded in the 4G Long Term Evolution (LTE) cellular signal for time synchronization in power grid monitoring, replacing the Pulse-Per-Second (PPS) signal that is retrieved from GPS receivers and being used by current monitoring systems. We implement our system over realistic smartphones with a few peripheral hardware, and realize a frequency monitoring accuracy of 0.2 mHz and a phase angle monitoring accuracy of 0.01 rad. Experiment results compared with the traditional Frequency Disturbance Recorders (FDRs) verify the effectiveness of our proposed system.**

***Index Terms*—Time synchonization, Long Term Evolution (LTE), Smartphone**

I. Introduction

Power grid is a critical infrastructure of the modern society, but is susceptible to various types of disturbances. When a significant disturbance occurs, the frequency and the phase angle of the power grid vary in both time and space, and, in many ways, exhibit the characteristics of electromechanical wave propagation phenomenon [1]. Therefore, the real-time awareness of phasor state could serve as a significant indicator of the power grid stability [2], and is indispensable for cyber-controlled smart grid construction.

How to obtain the phasor state more accurately and efficiently has been an active research topic for decades. Current power grid monitoring systems allow direct measurement of frequency and voltage phase angle by installing synchrophasors at either high-voltage transmission level [3] or low-voltage distribution level [4], [5]. These power grid monitoring systems, although having been proved to be effective in wide-area power grid infrastructure, are generally considered unsatisfactory for monitoring the operating status of the newly emerging distributed power systems, so-called microgrids [6]. Microgrids enable local integration of energy generation, distribution, and storage at the consumer level for better power system efficiency and control of demand [7]. The decentralization of microgrids poses higher requirements on the installation cost and accessibility of current synchrophasors, which are too expensive and inconvenient to be deployed into individual households in high volume. For example, the installation cost of one FDR is around $2,000, and it will cease to work when GPS signal is unstable or unavailable for indoor scenarios. This high cost and inconvenience would also reduce the end-users' incentives of having synchrophasors in their home energy systems.

In this paper, we present a practical system design which bridges the gaps between current power grid monitoring systems and the unique requirements of microgrid monitoring, by fully unleashing the capabilities of modern mobile platforms, particularly smartphones, in computation, communication, and storage. We proposed a novel time synchronization approach by harvesting the Primary Synchronization Signal (PSS) in the 4G LTE cellular radio, which significantly increases the system flexibility by eliminating the requirement of GPS reception and line of sight to the satellites. In addition, a low-cost monitoring prototype is implemented on the smartphone platform with a small quantity of peripheral hardware, which can be further integrated into the smartphone charger for better flexibility and convenience. The smartphone-based system lowers both the manufacturing and installation costs of the monitoring system. The accuracy of the frequency and phase angle measurements are 0.2 mHz and 0.01 rad, respectively.

The rest of this paper is organized as follows. Section II provides an overview of the system design. Section III presents our time synchronization approach based on harvesting the PSS signal from LTE radio. Section IV presents our performance evaluation in comparison with FDRs. Section V concludes the paper and discusses the future work.

II. Overview

In this section, we first briefly discuss our motivation of developing the power grid monitoring system over mobile platforms, particularly smartphones, and adopting the time signal from LTE for time synchronization. Afterwards, we present the hardware and software designs of our power grid monitoring system.

A. Motivation

1) Motivation for using mobile platforms: Modern mobile platforms, especially smartphones, are considered as ideal

This work was supported in part by the Engineering Research Center Program of the National Science Foundation and the Department of Energy under NSF Award Number EEC-1041877 and the CURENT Industry Partnership Program. Pending provisional patent has been filed by the University of Tennessee.

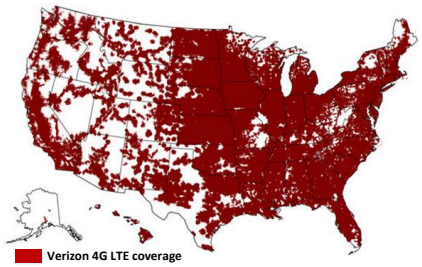

Fig. 1. The coverage of Verizon 4G LTE in US

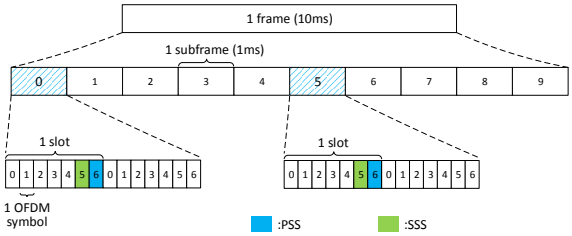

Fig. 2. Synchronization signals in LTE FDD downlink

choices to reduce the manufacturing cost of the power grid monitoring system. The essential components of a synchrophasor – powerful computation units, Internet access component and graphic interface component have all been provided by the modern smartphone platform. In particular, with the rapid development of IC and semiconductor manufacturing, the cost of a smartphone has been significantly reduced, and faster CPUs and more functionalities are integrated into the smartphone platform. For example, the Samsung Nexus S smartphone, with a price around 100 dollars, is equipped with 1 GHz ARM Cortex-A8 CPU, 512 MB RAM, GPS receiver (without analog PPS output), 4.0-inch LCD screen, WiFi connection and cellular network access. These capabilities make the modern smartphone platform be an ideal choice for implementing the microgrid monitoring systems.

2) Motivation for harvesting the time signal from 4G LTE radio: A globally synchronized clock with high accuracy and stability is required in the phase angle measurement. Simply speaking, a 15 milliseconds timing error, which is usually the upper bound of Network Timing Protocol (NTP) timing error, corresponds to an unacceptable measurement error of 330 degrees in a 60 Hz system. The PPS signal provided by the GPS system, with the accuracy in nanoseconds, are generally used in current synchrophasors systems. However, the GPS signal is usually unstable or unavailable in the indoor scenario where microgrids are usually operated. Therefore, a pervasive signal with the same level of accuracy is highly desired as an alternative of GPS. eLoran timing method [8] was successfully applied in synchrophasor measurement area and showed even better accuracy than GPS. However, eLoran timing method relies on high power transmitters, which results in high cost.

With its high data transmission rate and spectrum utilization efficiency, the 4G Long Term Evolution (LTE) has gained an extensive nationwide coverage, as shown in Fig. 1 [9], and is being widely deployed worldwide. An enhanced base station (eNodeB) of LTE is strictly synchronized with GPS or the Precision Time Protocol (PTP) [10]. The cell ID in

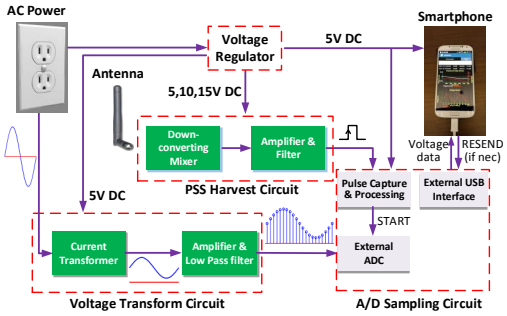

(a) System design

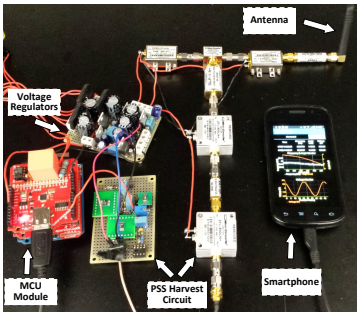

(b) System implementation

Fig. 3. Power grid monitoring over mobile platforms

the LTE network is then defined within two synchronization signals, namely Primary Synchronization Signal (PSS) and the Secondary Synchronization Signal (SSS). Fig. 2 illustrates the LTE frame format and the location of synchronization signals under Frequency-Division Duplexing (FDD) mode. The PSS signal repeats every 5 ms and therefore can be used as the time synchronization signal.

B. Hardware design

Our developed power grid monitoring system consists of voltage regulators, a voltage transform circuit, a microprocessor-controlled (MCU-controlled) AD sampling circuit, a PSS signal harvest module and an Android-based smartphone. The system design and implementation are shown in Fig. 3(a) and Fig. 3(b), respectively. The voltage regulator part outputs the DC power to power up the smartphone, MCU module and PSS harvest module. Current transformer takes an analog voltage signal from 120V wall outlet and transforms the AC power into the voltage range for analog-to-digital conversion (ADC) purpose. An 8-bit microprocessor ATmega328 (Arduino Uno board) is used to sample the voltage waveform through external AD converter at the sampling frequency of 1,440 Hz, and send the raw data to smartphone every 100 ms for processing.

The communication between the MCU and the smartphone is conducted by the USB host controller IC MAX3421E (USB host shield) [11]. The MAX3421E host controller contains the digital logic and analog circuitry necessary to implement a full-speed host compliant to USB specification v2.0. Under this circumstance, the smartphone behaves as USB slave in relation to the USB host chip, and can communicate with the MCU. The smartphone behaves as being connected to the desktop computer and will be charged while being connected to the USB host controller. The MCU communicates with the USB host shield through serial peripheral interface (SPI) bus.

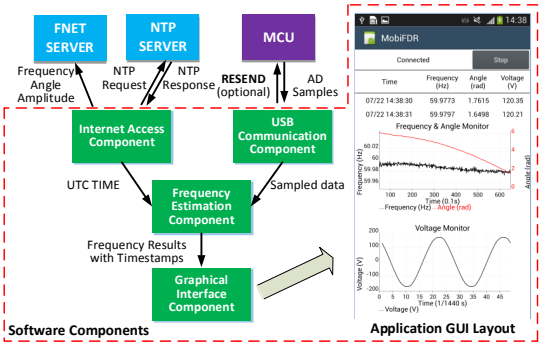

Fig. 4. Software components in the Android application

C. Software design

At the smartphone, the frequency estimation algorithm and visualization programs are packaged into one Android application. To keep the application responsive, the functionality of voltage data reception and the expensive computation of frequency estimation are distributed to an independent application thread, instead of residing in the application main thread or UI thread.

As shown in Fig. 4, our power grid monitoring application consists of four major components, which are explained in detail as follows:

1) **USB communication component.** Through the USB connection, the smartphone will receive the sampled measurement data from MCU. Our application will also monitor the connection status of the USB accessory. Once the smartphone is connected to the USB host controller with a correct hardware signature, our application will run automatically and build the USB connection as "plug-and-play".
2) **Frequency estimation component.** The phasor-based algorithms [12] estimating the power grid frequency and phase angles are implemented in this component.
3) **Internet access component.** Network access is necessary to obtain the NTP timing information and to upload the measurement results to the wide-area monitoring network Frequency Monitoring Network (FNET) operated by the University of Tennessee.
4) **Graphic interface component.** The information of frequency, phase angle and AC voltage are displayed at the smartphone for better user interaction. The graphic interface component is placed in the main thread.

III. Design Details

A. Harvesting the Primary Synchronization Signal (PSS)

The LTE cellular networks are the most advanced cellular communication infrastructure being deployed in the US, and its availability is rapidly increasing throughout the nation. In LTE networks, to achieve high data transmission rate, Orthogonal Frequency Division Multiple Access (OFDMA) is utilized as the physical layer technique in the downlink data transmission. The cell ID can be calculated as:

$$N_{ID}^{Cell} = 3N_{ID}^{1} + N_{ID}^{2} \tag{1}$$

where $N_{ID}^{1} \in 0, 1, ..., 167$ is the cell identity group and is located in SSS signal, and $N_{ID}^{2} \in 0, 1, 2$ is the cell identity and

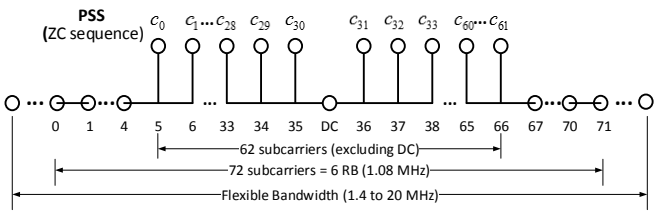

Fig. 5. Transmission of PSS signal in the frequency domain

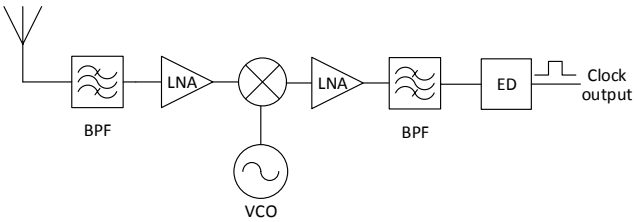

Fig. 6. System block diagram of the PSS signal harvesting circuit

is located in PSS signal. The SSS signal indicates the frame timing as they are different within a frame, while PSS signal indicates the OFDM symbol timing as they are the same within a frame. The sequence used for the PSS is generated from a frequency domain Zadoff-Chu (ZC) sequence according to [13]:

$$c_u(n) = \begin{cases} e^{-j\frac{\pi u n(n+1)}{63}} & n = 0, 1, ..., 30 \\ e^{-j\frac{\pi u(n+1)(n+2)}{63}} & n = 31, 32, ..., 61 \end{cases} \tag{2}$$

where the ZC root u for the PSS sequence is 25,29,34 that corresponds to the value of N_{ID}^{2} = 0,1,2, respectively.

Comprised with three Zadoff-Chu sequences in frequency domain, the PSS signal maps to the central 62 subcarriers around DC (within the central six Resource Blocks (RBs)), enabling the frequency mapping of the synchronization signals to be invariant with respect to the system bandwidth, which varies from 1.4 MHz to 20 MHz.

The frequency of PSS signal (200 Hz) is far less than the bandwidth of data transmitted (in the order of 1 MHz). Since our purpose of PSS detection is not to decode the signal but only to identify the arrival of the PSS signals, the PSS signal can be detected based on the scheme shown in Fig. 6. A Voltage-Controlled Oscillator (VCO) is used to detect the frequency band with the strongest signal strength. The signal in 1900 MHz frequency band is selected and downconverted to 200 kHz intermediate frequency (IF) output. The PSS signal would be transformed as a pulse after passing the bandpass filter with a bandwidth of 120 kHz and the envelope detector. The MCU will capture the rising edge of the PSS pulses as the trigger to start a new sampling cycle.

B. Coordination between smartphone and MCU

The major challenge of such coordination is that the local clock of the MCU will continuously drift due to the dynamic characteristics of the crystal oscillator, as well as various environmental factors such as temperature. As a result, the actual time period for each AC waveform sampling cycle may not be accurately set as expected. For example, a time period set to be the 100 ms by the MCU, which corresponds to the reporting rate in FNET, may be actually 99.8 ms or 100.1 ms due to the local clock drift. Such inaccurate

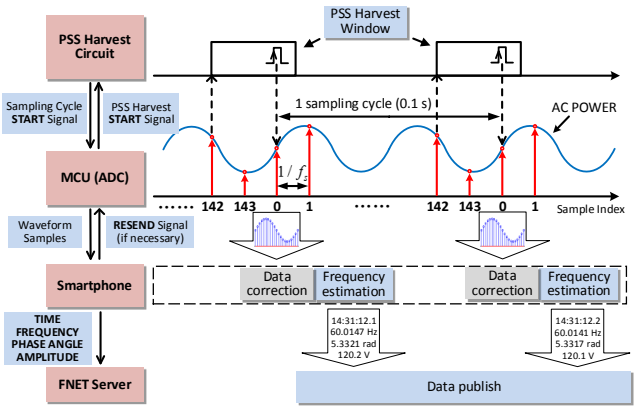

Fig. 7. System coordination between the smartphone and MCU

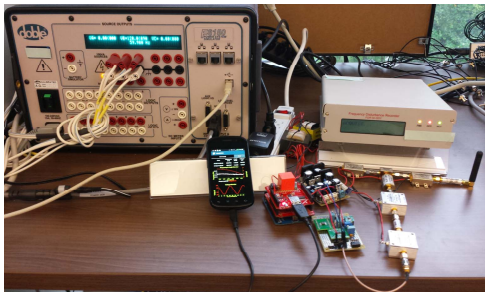

Fig. 8. Experiment setup

sampling frequency will result in the residue problem [14], i.e., the position of the first sample in one sampling cycle is different from that in another cycle, and the residue could be accumulated over time.

Our proposed method of determining the starting time of a new sampling cycle is shown in Fig. 7. Our monitoring system starts a new sampling cycle on every 100 ms, which is to be compatible with the reporting rate of the FNET network, and uses 1,440 Hz as the sampling frequency to ensure the measurement accuracy (12 or more data samples per period is needed in a 60 Hz power system). Correspondingly, 144 data samples are recorded in each sampling cycle. Our basic approach to addressing the above residue problem is to enable the PSS pulse detection after sampling the 142-nd samples (98.6ms) in current sampling cycle. The pulses received in this period cycle is assumed to be the PSS signal first, and the interval between the pulse and the last effective pulse is calculated. If the interval $\Delta t < \varepsilon$ where ε is the threshold, then the pulse is considered as an effective PSS output. The detection window will be closed and a new sampling cycle starts immediately. Otherwise, the pulse is assumed to be noise and if no effective pulses are detected in the detection window, the MCU will start a new sampling cycle at the time when sampling the 144th samples.

IV. Performance Evaluation

To evaluate the accuracy and effectiveness of the power grid monitoring of our proposed system, we test our system against the traditional FDR device. The system setup is shown in Fig. 8. The Doble F6150 power system simulator with GPS satellite synchronization is used to generate the standard AC power. The frequency and the phase angle accuracy of Doble F6150 simulator are 0.5 Part-Per-Million (PPM) and 0.1

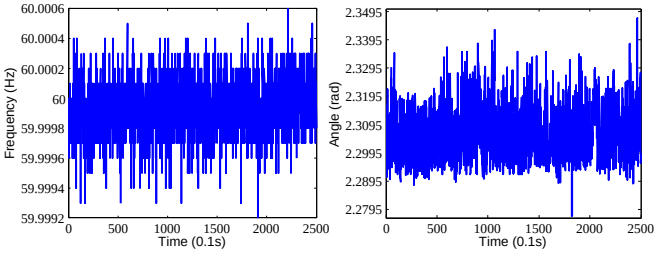

(a) Frequency (b) Phase angle

Fig. 9. Frequency and phase angle monitoring over 60 Hz Doble output

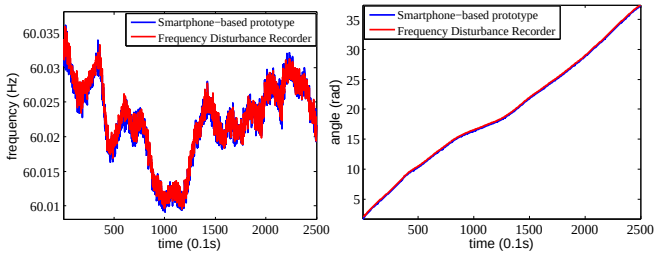

(a) Frequency (b) Phase angle

Fig. 10. Frequency and phase angle monitoring over 120V wall power

degree respectively. Both standard power generator and regular AC wall power are used in our experiments. In our prototype, the measurement results are written to a local textfile for review, while we extract the measurement results of FDR through FNET server.

A. Frequency and Angle measurement

First, the frequency measurement result over standard 60 Hz waveform generated by Doble is shown in Fig. 9. The error of the frequency measurement of our system is 0.2 mHz, compared with 0.22 mHz of the FDR device. For angle measurement, the standard deviation is used to evaluate the error. In the ideal condition, as to the waveform with fixed frequency, if 10 Hz reporting rate is applied, the curve of phase angle would be a straight line with fixed slope, in particular, a horizontal line under 60Hz condition. The standard deviation of the angle measurement result is 0.01 rad, which corresponds to 32us in 60 Hz system, compared to 0.002 rad of the FDR device. Second, the frequency measurement results over the 120V AC wall outlet are shown in Fig. 10. Our system is able to efficiently capture the trends of frequency deviations over time. Meanwhile, the difference between our system and the FDR measurements is 0.4 mHz. For angle measurement, since the PSS signal and the GPS signal are not precisely aligned, there is a nearly constant drift around the results. If eliminate the DC offset of two results, the difference between two curves is 0.011 rad.

In comparison with FDR, an 16-bit ADC used in our system lowers the quantization distortion in the AD process which leads to the increase of the frequency monitoring accuracy of the prototype. Angle measurement has a more strict demand on the clock accuracy than frequency measurement. Currently, the angle monitoring accuracy of our system is lower than that of FDR due to a couple of reasons. First, the timing error is introduced when capturing the PSS signal. The PSS signals are harvested in the form of pulses, and then the rising edge

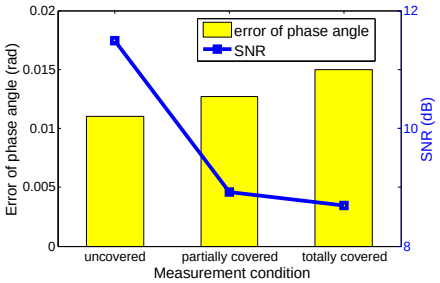

Fig. 11. Accuracy of phase angle measurement under different SNR of PSS signal

of the pulses will be captured by the MCU through external interrupt. Compared to the PPS pulses with a duration of 1.2 us and a steep rising edge, the slope of the rising edge of the PSS pulse is flatter and can be affected by the strength of the signal. Second, timing error exists in the timestamps compared to the real UTC time (GPS signal). That is, the time point of a frequency measurement is not exactly aligned with that of the GPS-based FDR. Different from GPS signal, there may be no PSS signal in the boundary of every two UTC seconds. Third, due to the involvement of both inductive and capacitive components such as transformers and analog filters with different time constants, possible phase lag or advance may be introduced into the frequency monitoring. This may induce a constant time deviance between measurements of our system and the FDR.

B. Measurement Accuracy vs. Signal-to-Noise Ratio

To evaluate the relationship between the measurement accuracy and the strength of the LTE cellular signal reception, we emulate the environment with different signal-to-noise ratio (SNR) by using aluminium foil to cover the antenna of the PSS harvest antenna. The complete coverage of the foil onto the antenna corresponds to the worst SNR environment. The performance of the phase angle measurement with respect to different SNR is depicted in Fig. 11. In Fig. 11, the PSS harvest module can achieve the highest SNR of 11.49 dB under no cover with the error of 0.01 rad on phase angle monitoring. As the coverage area of the foil increases, the error increases to 0.0127 and 0.015 rad in partially covered and totally covered situation, respectively. The reason of such a degradation partially results from the method of capturing the PSS pulses. As the noise level increases, the voltage amplitude of the PSS signal become closer to that of the noises, which refers to the slope of the rising edge of the PSS signal is small and susceptible to the noise. Since we regard the incoming of the rising edge of the PSS signal as the synchronization signal, the physical property of the MCU will introduce more uncertainty in a low SNR condition.

V. Conclusion and Future Work

In this paper, we presented the design and implementation of a GPS-free smartphone-based power grid frequency and angle monitoring system. In this system, we proposed to use the Primary Synchronization Signal in the 4G LTE cellular network as the synchronization source as an alternative of GPS signal. The extendability of the smartphone platform enables more functionalities to be further integrated into the system. The experiments compared with FDR devices verify the effectiveness of the system on frequency and angle monitoring. Our future work will focus on further improving the performance of PSS harvest module, simplifying the power grid monitoring system, and integrating more functionalities of power grid monitoring onto mobile platforms. First, we will modify the method in capturing the PSS signal by MCU. Instead of capturing the rising edge of the pulse, which is constrained by the property of the MCU circuitry and of more uncertainty in a low SNR condition, a high-speed ADC will be used to collect the waveform of the IF signal, and the peak detection algorithms would be applied to the IF signal to detect the peak of PSS pulse as the start of a sampling cycle. Second, we will fabricate all the external components including MCU board, PSS harvest module and the voltage transform circuit into one PCB board, so that our monitoring system could be integrated into the smartphone charger for better accessibility. Third, our system will be further extended to incorporate more functionalities such as power quality measurement that monitors power grid operations in a much wider range of frequency spectrum.

References

[1] J. S. Thorp, C. E. Seyler, and A. G. Phadke, "Electromechanical wave propagation in large electric power systems," *Circuits and Systems I: Fundamental Theory and Applications, IEEE Transactions on*, vol. 45, no. 6, pp. 614–622, 1998.

[2] H. Karimi, M. Karimi-Ghartemani, and M. R. Iravani, "Estimation of frequency and its rate of change for applications in power systems," *IEEE Transactions on Power Delivery*, vol. 19, no. 2, pp. 472–480, 2004.

[3] V. Venkatasubramanian, H. Schattler, and J. Zaborszky, "Fast time-varying phasor analysis in the balanced three-phase large electric power system," *IEEE Transactions on Automatic Control*, vol. 40, no. 11, pp. 1975–1982, 1995.

[4] Y. Zhang, P. Markham, T. Xia, L. Chen, Y. Ye, Z. Wu, Z. Yuan, L. Wang, J. Bank, J. Burgett *et al.*, "Wide-area frequency monitoring network (FNET) architecture and applications," *IEEE Transactions on Smart Grid*, vol. 1, no. 2, pp. 159–167, 2010.

[5] L. Zhan and Y. Liu, "Improved wls-tf algorithm for dynamic synchronized angle and frequency estimation," in *PES General Meeting — Conference Exposition, 2014 IEEE*, July 2014, pp. 1–5.

[6] C. W. Gellings, M. Samotyj, and B. Howe, "The future's smart delivery system," *IEEE Power and Energy Magazine*, vol. 2, no. 5, pp. 40–48, 2004.

[7] F. Giraud and Z. M. Salameh, "Steady-state performance of a grid-connected rooftop hybrid wind-photovoltaic power system with battery storage," *IEEE Transactions on Energy Conversion*, vol. 16, no. 1, pp. 1–7, 2001.

[8] L. Zhan, D. Zhou, T. King, Y. Liu, E. Johannessen, J. Alexander, and B. Boza, "Improvement of timing reliability and data transfer security of synchrophasor measurements," in *T D Conference and Exposition, 2014 IEEE PES*, April 2014, pp. 1–5.

[9] Verizon Wireless, "LTE network coverage 2014," http://www.verizonwireless.com/wcms/consumer/4g-lte.html.

[10] "IEEE standard for a precision clock synchronization protocol for networked measurement and control systems," *IEEE Std 1588-2008 (Revision of IEEE Std 1588-2002)*, pp. c1–269, July 2008.

[11] MAXIM Integrated (2007), "MAX3421E, usb peripheral/host controller with spi interface," copyright Maxim Integrated Products.

[12] A. G. Phadke, J. S. Thorp, and M. G. Adamiak, "A new measurement technique for tracking voltage phasors, local system frequency, and rate of change of frequency," *IEEE Transactions on Power Apparatus and Systems*, no. 5, pp. 1025–1038, 1983.

[13] 3rd Generation Partnership Project (3GPP); Technical Specification Group Radio Access Network, "Evolved universal terrestrial radio access (E-UTRA); physical channels and modulation (release 10) TS 36.211 (version 10.0.0)," Tech. Rep., 2010.

[14] J. Zuo, "The frequency monitor network (FNET) design and situation awareness algorithm development," Ph.D. dissertation, Virginia Polytechnic Institute and State University, 2008.